

Limit Cycle Oscillations of a Complete Aircraft

Mayuresh J. Patil,* Dewey H. Hodges[†]

Georgia Institute of Technology, Atlanta, Georgia.

and

Carlos E. S. Cesnik[‡]

Massachusetts Institute of Technology, Cambridge, Massachusetts

Abstract

This paper presents results for the aeroelastic stability and LCO behavior for a complete aircraft. Comparison are presented between the results predicted by a cantilevered wing model, an untrimmed aircraft model (no gravity or drag) and a trimmed aircraft model. It is seen that the stability behavior is predicted accurately only if the correct trim loads are applied to the wing. The LCO behavior of the untrimmed aircraft was similar to that of the cantilevered wing. On the other hand, the LCO behavior of the trimmed aircraft configuration was complicated due to the presence of flight dynamic instabilities.

Introduction

An earlier paper by the authors (Patil *et al.* 1999) presents results obtained for limit-cycle oscillations (LCOs) in high-aspect-ratio wings due to structural (geometric) and aerodynamic (stall) nonlinearities. The analysis is based on geometrically-exact structural analysis and finite-state unsteady aerodynamics with stall. The results indicate that stall limits the amplitude of post-flutter unstable oscillations. Even at speeds below the linear flutter speed, LCOs can be observed if the stable steady

state is disturbed by a finite-amplitude disturbance. The present paper seeks to extend the methodology and results obtained earlier to complete aircraft.

The motivation for the present work is twofold. Firstly, the LCO will be affected by aircraft motion and the aircraft motion will be affected by the LCO. Thus, the LCO predicted by a cantilevered wing will not accurately predict the actual behavior of a wing on an aircraft in flight especially for HALE-type aircraft where the mass of the fuselage is low, leading to large motion of the aircraft; and the frequencies of the wing are low, leading to stronger coupling with flight dynamics. Also, the amplitude of vibrations of the fuselage is of significance because the sensors will have to function accurately under these vibrations. Secondly, LCO prediction of a cantilevered wing assumes that the aircraft continues its motion with the velocity specified; whereas, in actual flight due to the wing instability/motion and the associated unsteady drag (or propulsion of oscillating wing), the aircraft flight condition will change. Thus, the assumption that the engine will continue to provide the propulsive forces required to maintain assumed speed is incorrect. A realistic assumption is that the propulsive force is constant and the velocity of the aircraft may change with changes in flight condition. Such an analysis with a constant power source will further help understand post-flutter phenomena and pre-flutter LCO phenomena in actual aircraft.

Background

The linear theory of stability, when applied to aeroelasticity problems, typically leads to a set of eigenvalues. It predicts that small disturbances applied to a system at an unstable equilibrium grow

*Post-Doctoral Fellow, School of Aerospace Engineering.
Member, AIAA.

[†]Professor, School of Aerospace Engineering.
Fellow, AIAA. Member, AHS.

[‡]Asst. Professor, Dept. of Aeronautics and Astronautics.
Senior Member, AIAA. Member AHS.

Copyright ©2000 by Mayuresh Patil, Dewey Hodges and Carlos Cesnik. Published by the American Institute of Aeronautics and Astronautics, Inc. with permission.

exponentially. Within its valid range, linear theory is correct, *i.e.*, *small* disturbances *do* grow exponentially – at least *at first*. However, one should not regard the results of linear theory to have any significance whatsoever regarding the behavior of a system subjected to large disturbances, or after a long time elapses from an initial small disturbance. For example, according to linear theory the response of an unstable system will diverge from the unstable equilibrium to infinity (or material failure). This does not always comport with experimental evidence, and nonlinear analysis methodology has been developed to remedy this problem. Moreover, an LCO is not necessarily the result of a linear instability. LCOs can be induced by certain disturbances, if sufficiently large, even when the given equilibrium state is stable. Basically, if the disturbances are not small, then the response cannot be predicted by theories that are linearized about a nonlinear steady state.

If a system has a nonlinear stiffening term, then in most occasions the amplitude of oscillations will grow until an LCO is reached. LCOs, though stable in the sense of Lyapunov, are not asymptotically stable. That is, although the final state is bounded, the system will not asymptotically approach its original equilibrium state as time grows. Depending on the amplitude of the LCO, the structure may or may not experience immediate failure. However, for an aircraft, LCOs pose significant problems in their own right. The vibration caused by LCOs causes fatigue, reducing the useful life of the structure. Thus, efficient prediction of LCOs is very important during design, especially for aircraft flying near the limits of the linear assumptions.

There are two main motivating factors for the present study, *i)* to investigate LCO in aircraft with high-aspect-ratio wings, (like those to be used in future high-altitude, long-endurance, unmanned aerial missions,) using time response analysis, and, *ii)* to investigate mechanisms responsible for LCO of a complete aircraft and the role of limited propulsive power.

Literature Survey

There are various modalities to analyze and predict LCO, the most common methodology being time marching. The system is simulated in time for various initial conditions. And the response is plotted in time or as a phase-plane plot to see if *i)* the response

is diverging and *ii)* it converges to an LCO. This is very much computer time intensive and one needs to select a set of initial conditions relevant to the problem at hand. Tang *et al.*(1998) used a reduced-order, finite-state inflow model to analyze the nonlinear behavior of airfoil sections with free play nonlinearities. Tang and Dowell (1993) have analyzed the nonlinear behavior of a flexible rotor blade due to structural free-play and aerodynamic stall nonlinearities. The analytical results were compared with experimental observations. In both cases time-marching was used. Patil *et al.*(1999) have presented results on the LCO observed in a high-aspect-ratio cantilevered wing. Finite elements in space and time were used for time integration. This present paper is an extension to a complete aircraft LCO. Recently, there has also been some work in coupling computational fluid dynamics (CFD) and computational structural dynamics (CSD) models for prediction of LCO of fighter wing configurations in transonic flow, *e.g.*, Smith and Huttshell (1999).

In harmonic balance analysis the response is assumed to be a linear combination of a set number of harmonics. The solution is obtained by solving the nonlinear algebraic equations associated with all the harmonics. Dunn and Dugundji (1992) used Fourier analysis to extract the relevant harmonics from the ONERA dynamic stall model and then used the harmonic balance method to predict LCOs in a plate-like composite wing. The results obtained were compared with experimental data.

Experimental data for an airfoil on a nonlinear support system has been obtained by O’Neil and Strganac (1996). A later theoretical analysis using the method of multiple scales by Gilliatt *et al.*(1998) includes nonlinearities due to stall in a quasi-steady way. The objective was to predict internal resonance in such a model and to explore its effect as an LCO-triggering mechanism.

Aeroelastic Model

The aeroelastic model used in the present analysis is based on two separate works, *viz.*, *i)* mixed variational formulation based on exact intrinsic equations for dynamics of beams in a moving frame (Hodges 1990) and *ii)* finite-state airloads for deformable airfoils on fixed and rotating wings (Peters and Johnson 1994, Peters *et al.* 1995). The structural theory

is a nonlinear intrinsic formulation for the dynamics of initially curved and twisted beams. There are no approximations to the geometry of the reference line of the deformed beam or to the orientation of the cross-sectional reference frame of the deformed beam. A compact mixed variational formulation can be derived from these equations which is well-suited for low-order beam finite element analysis based in part on the paper by Hodges (1990). The aerodynamic model consists of a state-space theory for the lift, drag, and all generalized forces of a deformable airfoil. Trailing edge flap deflections are included implicitly as a special case of generalized deformation. The theory allows for a thin airfoil which can undergo arbitrary small deformations with respect to a reference frame which can perform arbitrarily large motions. For

In the present work, rigid-body (beam root) degrees-of-freedom are added to the formulation so as to simulate the fuselage motion. Also, gravitational potential is added to the potential energy expression used in the Hamilton's principle which generates the equations of motion. Coupling the structural and aerodynamics models, one obtains a complete aeroelastic model. Finite elements in space and time are used to march in time and get the dynamic nonlinear behavior of the system. The formulation is given in detail in by Patil (1999).

Preliminary results

The model used here to illustrate the overall aircraft behavior is a HALE-like aircraft with high-aspect-ratio wings (half-span aspect ratio of 12). Table 1 gives the model parameters. Results are presented for three cases, *i*) cantilevered wing, *ii*) aircraft model including the rigid-body modes (no trim) and *iii*) complete trimmed aircraft. First stability prediction are presented for the three cases, followed by LCO results and finally, some flight dynamics response results are presented.

Stability Results

For the cantilevered wing the flutter speed of the undeformed wing was calculated. The calculations do not include gravity and drag forces and thus represents linear results. The flutter speed is 29.96 m/s and the corresponding flutter frequency is 26.98

rad/s. Flutter calculations are conducted using eight finite elements for structural (and aerodynamic) representation and six inflow states at each aerodynamic station.

Now lets consider case (*ii*). Including the rigid-body aircraft degrees of freedom in the stability analysis does not change instability speed very much for the present model. Again, these calculations are conducted without including drag and gravity. Thus, such modeling leads to easy inclusion of flight dynamic modes without the complexity of trimming a flexible aircraft. These calculations are conducted for various ratios of fuselage mass to wing mass. For the nominal case of the fuselage mass being 2.5 times the wing mass, the flutter speed is 29.90 m/s and the flutter frequency is 26.86 rad/s. Comparing with the flutter results for simple cantilevered wing we see that the difference is quite small. Fig. 1 shows the change in flutter speed with change in the mass ratio. As can be expected, as the fuselage mass is increased the behavior of the wing is decoupled from the fuselage and the response approaches that of the cantilevered wing. On the other hand, for low fuselage mass, there is a significant decrease in the flutter speed.

Finally, lets turn our attention to the trim results. Trimming a flexible aircraft with large wing deformations (*i.e.*, including nonlinear effects) is quite challenging. A symmetric flight condition is assumed in the presented results and gravity as well as drag forces are included. A trim condition is established by controlling the aircraft angle-of-attack, the thrust developed by the engine and the elevator deflection on the horizontal stabilizer. A trim analysis based on Newton-Rhapson method was developed which releases one constrain at a time and tries to zero-out the corresponding aircraft velocity by manipulating the controls. The flutter speed for the trimmed aircraft is 26.9 m/s and the flutter frequency is 21.3 rad/s. This is a drastic decrease in the flutter speed as compared to the instability speed predicted for a cantilevered wing as well as the untrimmed aircraft. This change in the aeroelastic characteristics of the wing can be attributed to the change in the structural characteristics of the wing due to deformation. Trimming the aircraft leads to an accurate estimation of the loads on the wing, the corresponding deformation and the nonlinear effects (see Patil *et al.*(1999) for more explanation). Fig. 2 shows the plot of damping of the critical flutter mode as a function of velocity for the

three cases considered (assuming nominal fuselage to wing mass ratio of 2.5). Interestingly enough, there is not much difference in the behavior of the complete untrimmed aircraft as compared to that of the cantilevered wing suggesting minimal involvement of the rigid-body modes in the aeroelastic (flexible) response. The trimmed aircraft results are quite different as expected due to the structural nonlinearities.

Limit Cycle Oscillations

As given in the earlier section the flutter speed for all three cases is less than 30 m/s. The wing/aircraft at 32 m/s is given small disturbance about its equilibrium/trim state and the time history is plotted to reveal the post-flutter response of the wing/aircraft.

Fig. 3 shows the time history of tip displacement and rotation for a cantilevered wing. As expected stall limits the amplitude of oscillations leading to limit cycle oscillations. The interesting fact is that though the amplitude of oscillations stops increasing, the mode of oscillation continues to change. The LCO is not sinusoidal. The pitch response has higher harmonic content. Also, the bending oscillations which start off oscillating about the mean undeformed position shift to oscillations about a deformed shape. The reason is possible due to the generation of net lifting force due to the non-sinusoidal oscillations. This net lifting force leads to a mean wing deformation.

Fig. 4 shows the plot of tip displacement and rotation for response of the untrimmed aircraft. Here only the aircraft pitch and plunge modes are unrestrained. Again the oscillations reach a limited amplitude motion. Here the amplitude of oscillations is lower as compared to the cantilevered wing. The LCO has a small amount of higher harmonic content in the pitch response. Fig. 4 also shows the plot of the aircraft fuselage velocity and angular velocity. As can be seen there is a participation of the rigid body modes in the LCO phenomenon.

Fig. 5 shows the time history of various variable for a trimmed aircraft. As can be seen the response is quite different as compared to that of the untrimmed aircraft. There is a lightly-damped, low-frequency flight dynamic mode which affects the aircraft motion in addition to the effect of the flutter mode. As

can be seen from the plot, there is increase in the wing response due to flutter. But, there is also a flight dynamic instability which drives the aircraft to nose dive. During the nose dive the aircraft gains speed and thus there is a gradual increase in the LCO amplitude. Flight dynamic instabilities complicate the complete aircraft (trimmed or untrimmed) LCO analysis. The small disturbance in rigid-body/flight-dynamics modes take a long time to decay and that leads to large changes in the flight response. Such flight dynamic modes should be controlled by having an online flight control system which stabilizes the aircraft flight dynamics.

Flight Response Predictions

The analysis tool developed can also be used for flight dynamics simulation of a flexible aircraft. Since the structural geometric nonlinearities and aerodynamic stall nonlinearities are included, the present analysis tool is ideal for predicting large angle flight maneuver as well as for flight response after a system failure. In this paper, an example is presented which gives an idea as to the usefulness of the present analysis. Flight response of the aircraft to small disturbances below the flutter speed is presented next. Here, the nominal speed is assumed to be 25 m/s.

Fig. 6 shows the vertical and horizontal velocity response of the aircraft to a small disturbance. Here it should be noted that the time scale is much larger as compared to the flutter response plots. As can be seen the flight dynamic mode has a low frequency and is lightly damped.

Conclusions

The phenomenon of limit-cycle oscillation has been numerically studied for a complete aircraft with high-aspect-ratio cantilevered wing. The results account for structural and aerodynamic nonlinearities through the use of a geometrically-exact beam analysis and finite-state unsteady aerodynamics with stall. Three cases were considered, *viz.*, *i)* cantilevered wing, *ii)* aircraft including the rigid-body modes, and *iii)* complete trimmed aircraft. Stability results show the similarities as well as differences between the three cases. The rigid-body dynamics interactions with aeroelastic phenomenon was not strong. On the other hand, trimmed aircraft analysis leads

to very different results since trimmed aircraft analysis takes into account the trim deflected shape of the wing and thus accounts for any structural geometric nonlinearities.

As expected, the results show that stall limits the amplitude of post-flutter unstable oscillations for the wing as well as the complete aircraft. The LCO behavior for the three cases was quite different. This indicates the need for conducting LCO calculations on a trimmed aircraft rather than a cantilevered wing. To reduce the effect of low-frequency lightly-damped flight dynamic modes a flight controller should be implemented so as to keep the overall flight response stable. Further studies are needed to predict the existence of pre-flutter LCO. Such LCO's have been shown for cantilevered wings and are likely to occur in complete aircraft aeroelasticity. Finally, a better high angle-of-attack drag model is required to accurately predict the post-flutter response of the aircraft when the propulsive force is held constant.

Acknowledgments

This work was supported by the U.S. Air Force Office of Scientific Research (Grant number F49620-98-1-0032), the technical monitor of which is Maj. Brian P. Sanders, Ph.D.

References

- [1] Dunn, P. and Dugundji, J., "Nonlinear Stall Flutter and Divergence Analysis of Cantilevered Graphite/Epoxy Wings," *AIAA Journal*, Vol. 30, No. 1, Jan. 1992, pp. 153 – 162.
- [2] Gilliatt, H. C., Strganac, T. W., and Kurdila, A. J., "On the Presence of Internal Resonances in Aeroelastic Systems," In *Proceedings of the 39th Structures, Structural Dynamics, and Materials Conference*, Long Beach, California, April 1998, pp. 2045 – 2055.
- [3] O'Neil, T. and Strganac, T. W., "Nonlinear Aeroelastic Response - Analyses and Experiments," In *Proceedings of the 34th Aerospace Sciences Meeting and Exhibit*, Reno, Nevada, Jan 1996, AIAA-96-0014.
- [4] Hodges, D. H., "A Mixed Variational Formulation Based on Exact Intrinsic Equations for Dynamics of Moving Beams," *International Journal of Solids and Structures*, Vol. 26, No. 11, 1990, pp. 1253 – 1273.
- [5] Patil, M. J., *Nonlinear Aeroelastic Analysis, Flight Dynamics, and Control of a Complete Aircraft*, Ph.D. Thesis, Georgia Institute of Technology, Atlanta, Georgia, May 1999.
- [6] Patil, M. J., Hodges, D. H., and Cesnik, C. E. S., "Nonlinear Aeroelasticity and Flight Dynamics of High-Altitude Long-Endurance Aircraft," In *Proceedings of the 40th Structures, Structural Dynamics and Materials Conference, Saint Louis, Missouri*, April 12 – 15, 1999, pp. 2224 – 2232, AIAA Paper 99-1470.
- [7] Patil, M. J., Hodges, D. H., and Cesnik, C. E. S., "Limit Cycle Oscillations in High-Aspect-Ratio Wings," In *Proceedings of the 40th Structures, Structural Dynamics and Materials Conference, Saint Louis, Missouri*, April 12 – 15, 1999, pp. 2184 – 2194, AIAA Paper 99-1464.
- [8] Peters, D. A. and Johnson, M. J., "Finite-State Airloads for Deformable Airfoils on Fixed and Rotating Wings," In *Symposium on Aeroelasticity and Fluid/Structure Interaction, Proceedings of the Winter Annual Meeting*. ASME, November 6 – 11, 1994.
- [9] Peters, D. A., Barwey, D., and Johnson, M. J., "Finite-State Airloads Modeling with Compressibility and Unsteady Free-Stream," In *Proceedings of the Sixth International Workshop on Dynamics and Aeroelastic Stability Modeling of Rotorcraft Systems*, November 8 – 10, 1995.
- [10] Smith, M. J. and Huttshell, L. J., "Computational Evaluation of Semispan Straked Delta Wing Flowfields Conducive to LCO," In *Proceedings of the 40th Structures, Structural Dynamics and Materials Conference, Saint Louis, Missouri*, April 12 – 15, 1999, AIAA Paper 99-1212.
- [11] Tang, D. M. and Dowell, E. H., "Experimental and Theoretical Study for Nonlinear Aeroelastic Behavior of a Flexible Rotor Blade," *AIAA Journal*, Vol. 31, No. 6, June 1993, pp. 1133 – 1142.
- [12] Tang, D., Conner, M. D., and Dowell, E. H., "Reduced-Order Aerodynamic Model and Its Application to a Nonlinear Aeroelastic System," *Journal of Aircraft*, Vol. 35, No. 2, Mar – Apr 1998, pp. 332 – 338.

WING	
Half span	12 m
Chord	1 m
Mass per unit length	1.0 kg/m
Mom. Inertia	0.134 kg m
Spanwise elastic axis	35% chord
Center of gravity	45% chord
Bending rigidity	5×10^4 N m ²
Torsional rigidity	1×10^4 N m ²
Bending rigidity (chordwise)	5×10^6 N m ²
PAYLOAD & TAILBOOM	
Mass	60 kg
Moment of Inertia	300 kg m ²
Length of tail boom	8 m
TAIL	
Half span	2.5 m
Chord	1 m
Mass per unit length	0.08 kg/m
Moment of Inertia	0.01 kg m
Center of gravity	50 % of chord
FLIGHT CONDITION	
Altitude	10 km
Density of air	0.41351 kg/m ³

Table 1: Aircraft model data

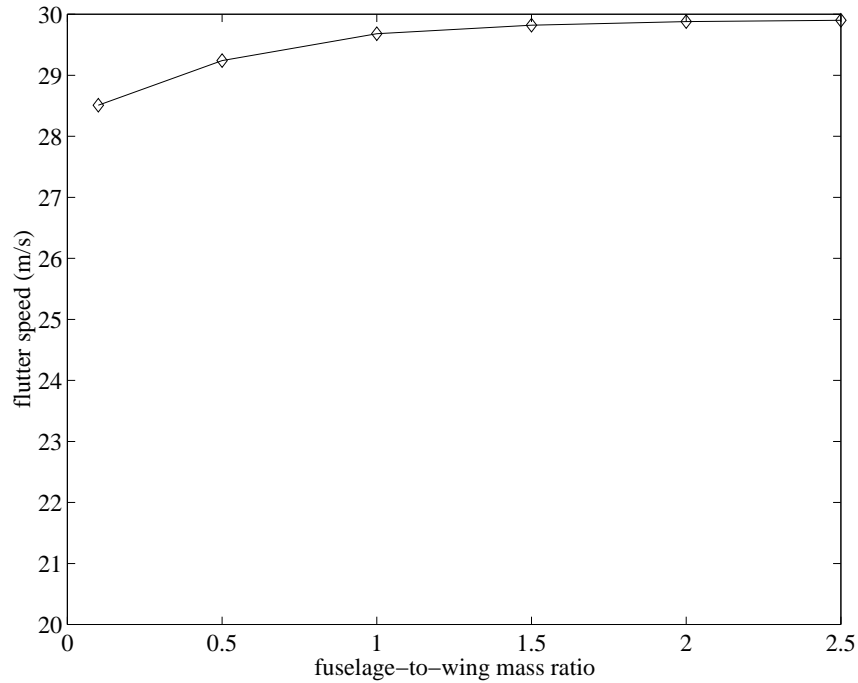


Figure 1: The effect of fuselage-to-wing mass ratio on the flutter speed of an untrimmed aircraft

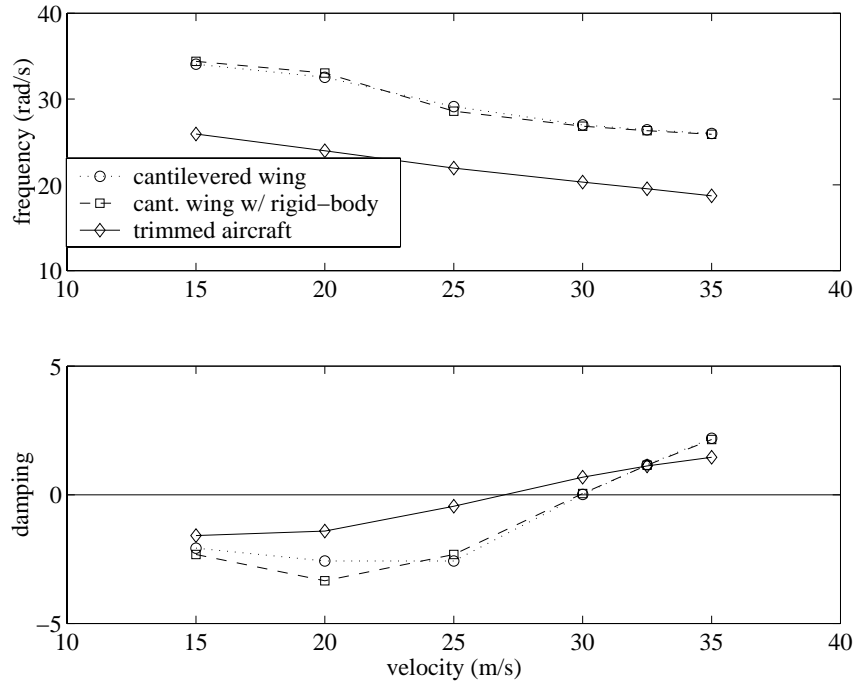


Figure 2: The frequency and damping of the critical (flutter mode) predicted for the three cases

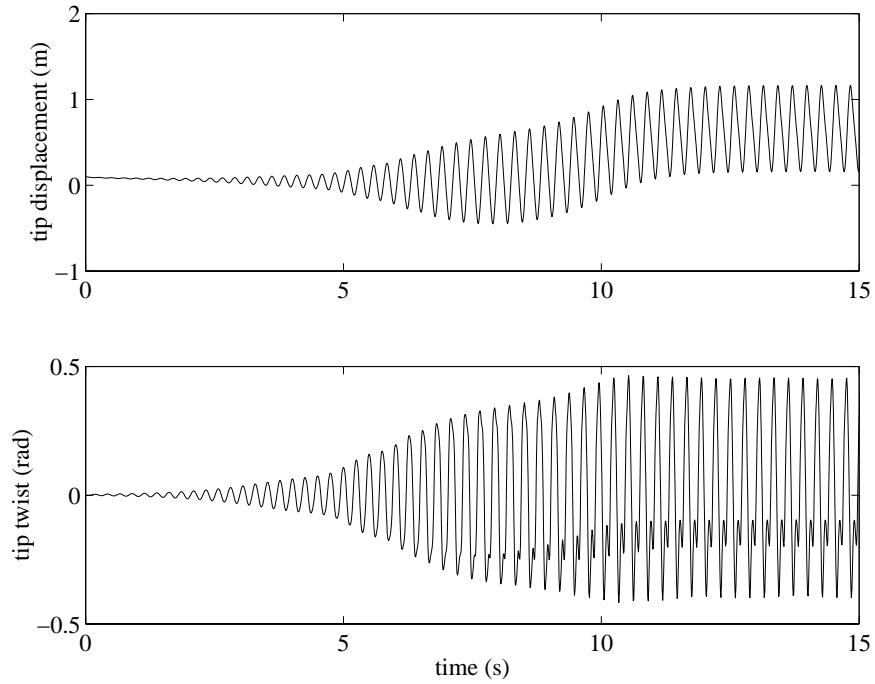


Figure 3: LCO result for the cantilevered wing (speed = 32 m/s)

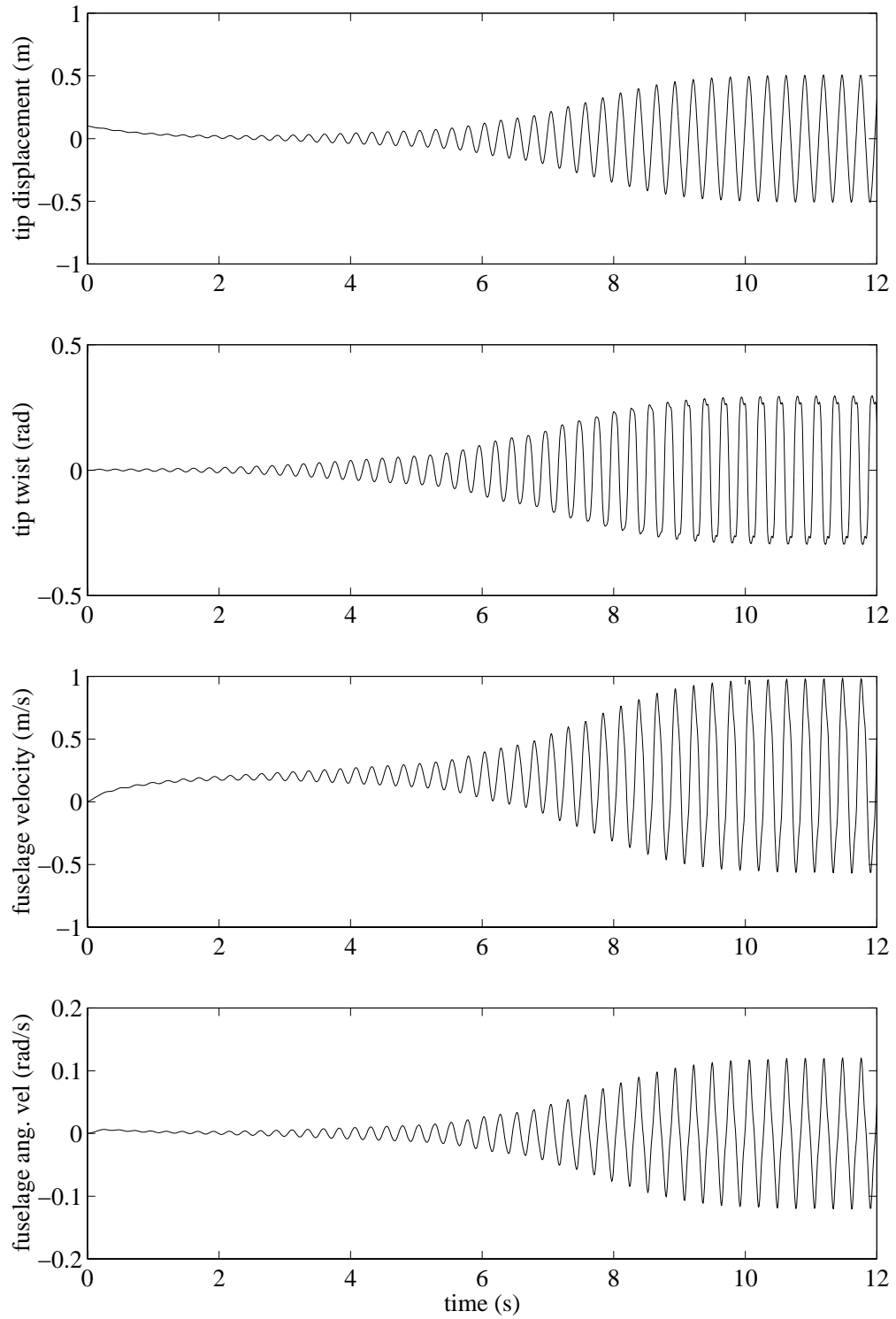


Figure 4: LCO result for the untrimmed aircraft (speed = 32 m/s)

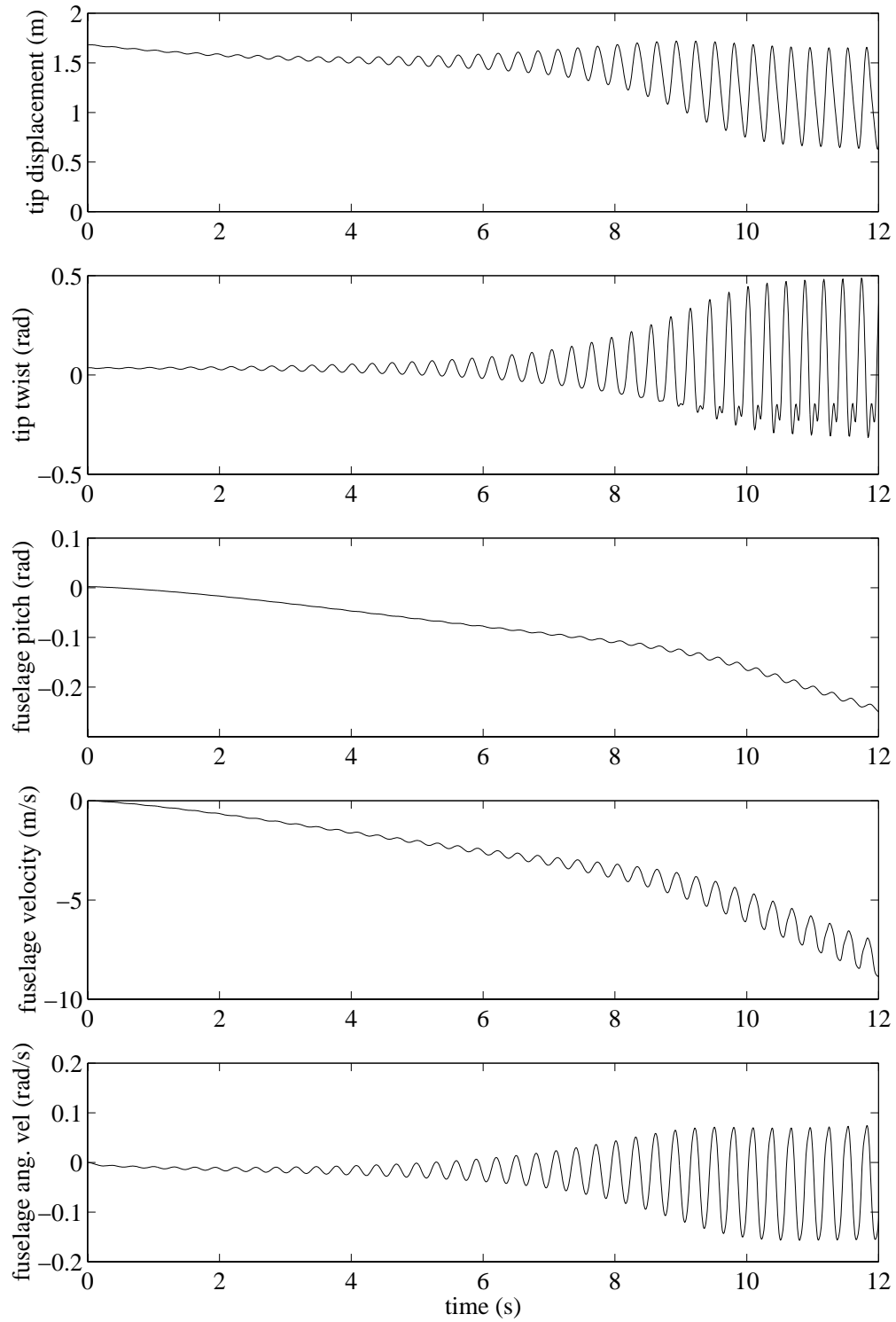


Figure 5: LCO result for the complete trimmed aircraft (speed = 32 m/s)

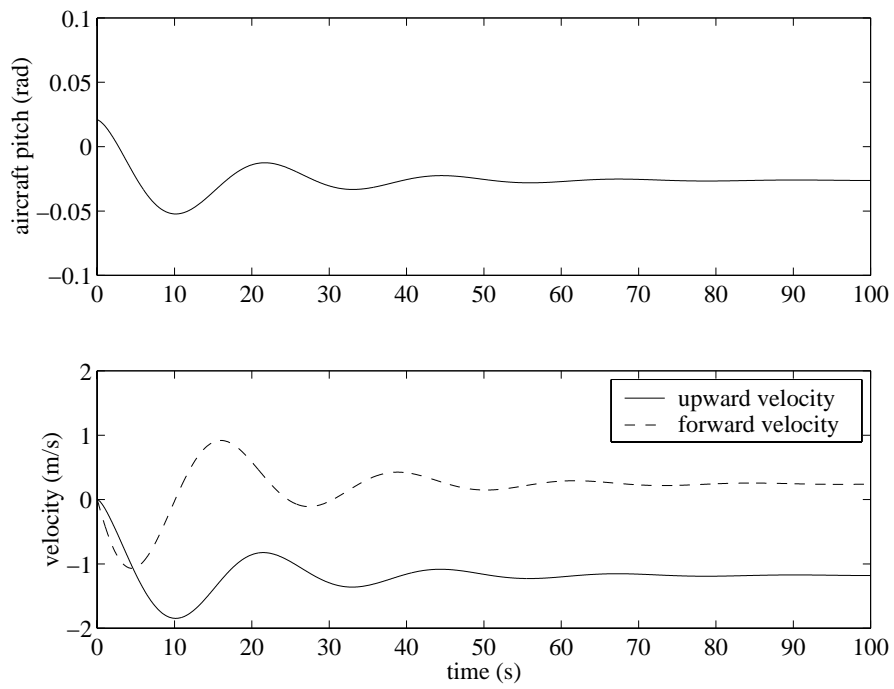


Figure 6: Low-frequency aircraft response (speed = 25 m/s)